Patterns and genomic correlates of PD-L1 expression in patients with biliary tract cancers

Kabir Mody[1], Jason Starr[1], Michelle Saul[2], Kelsey Poorman[2], Benjamin A. Weinberg[3], Mohamed E. Salem[4], Ari VanderWalde[5], Anthony F. Shields[6]

[1]Gastrointestinal Oncology Program, Division of Hematology/Oncology, Mayo Clinic, Jacksonville, FL, USA; [2]Caris Life Sciences, Phoenix, AZ, USA; [3]Ruesch Center for The Cure of Gastrointestinal Cancers, Lombardi Comprehensive Cancer Center, Georgetown University Medical Center, Washington, DC, USA; [4]Levine Cancer Institute, Carolinas HealthCare System, Charlotte, NC, USA; [5]West Cancer Center, Division of Hematology and Oncology, Department of Medicine, University of Tennessee, Memphis, TN, USA; [6]Department of Oncology, Karmanos Cancer Institute, Wayne State University, Detroit, MI, USA

Contributions: (I) Conception and design: K Mody; (II) Administrative support: None; (III) Provision of study materials or patients: K Mody, K Poorman, J Starr; (IV) Collection and assembly of data: K Mody, K Poorman, J Starr; (V) Data analysis and interpretation: K Mody, K Poorman, ME Salem, J Starr; (VI) Manuscript writing: All authors; (VII) Final approval of manuscript: All authors.

Correspondence to: Kabir Mody, MD. Gastrointestinal Oncology Program, Division of Hematology/Oncology, Mayo Clinic Cancer Center, Mayo Clinic, 4500 San Pablo Rd, Jacksonville, FL 32224, USA. Email: mody.kabir@mayo.edu.

Background: Patients with biliary tract cancer (BTC) have a dismal prognosis and limited treatment options. Given the potential for immunotherapy in patients with BTC, we studied the expression of programmed death ligand-1 (PD-L1)/programmed death-1 (PD-1) and evaluated for associated genetic alterations in patients with BTC.

Methods: By immunohistochemistry (IHC), PD-L1 (SP142 antibody; ≥2+ and/or ≥5% staining on tumor cells considered positive) and PD-1 [NAT105 antibody; ≥1+ staining of tumor infiltrating lymphocytes (TILs) considered positive] expression was studied and next-generation sequencing (NGS) was performed using Caris Life Sciences' sequencing panel of 592 genes. A total of 652 patients with BTC were included in this study: 77 extrahepatic cholangiocarcinoma (ECC), 203 gallbladder cancer (GBC), and 372 intrahepatic cholangiocarcinoma (ICC).

Results: Of the 652 tumors 8.6% were PD-L1 positive with the following distribution: GBC 12.3% (25/203), ICC 7.3% (27/372), and ECC 5.2% (4/77). There was a statistically significant increase in BRAF, BRCA2, RNF43, and TP53 mutations in PD-L1 positive group as compared to PD-L1 negative. Among other biomarkers tested, TOP2A, tumor mutational burden (TMB) high (≥17 mutations per megabase) (10.7%), and microsatellite instability high (MSI-H) (7.1%) were increased in PD-L1 positive tumors versus PD-L1 negative tumors.

Conclusions: PD-L1 expression was noted in a small percentage (8.6%) of patients with BTC. This finding suggests potential benefit of immunotherapy in this subset of patients. Furthermore, there was a statistically significant association between PD-L1 expression and certain genomic alterations (*BRAF*, *BRCA2*, *RNF43*, *TP53*) and biomarkers (TOP2A, TMB high, MSI-H), which might direct the use of rational combination strategies and clinical trial development.

Keywords: Cholangiocarcinoma; immunotherapy; mutation; bile ducts; intrahepatic; bile ducts; extrahepatic; gallbladder cancer (GBC).

1100

Mody et al. PD-L1 expression correlates in BTC

Introduction

Biliary tract cancer (BTC) is a malignancy derived from the epithelial cells lining the biliary tree (1). In the United States, BTC accounts for 2% of all new cancer diagnoses and the incidence continues to rise (2-5). In the last four decades, the incidence rates in US of intrahepatic BTC have increased by 165% (2-6). Unfortunately, BTC is a lethal malignancy and often presents in advanced stages. Treatment options are limited and gemcitabine/cisplatin remains the standard therapy with improved median overall survival (mOS) (11.7 *vs.* 8.1 months) and median progression-free survival (mPFS) (8.0 *vs.* 5.0 months) compared to gemcitabine alone (7). Given these outcomes, there is a dire need for novel, more effective and personalized treatment strategies.

BTCs can be split into 4 subtypes based on their location, classified as intrahepatic, extrahepatic (hilar and distal) cholangiocarcinoma, and gallbladder cancer (GBC). These subtypes now have been further characterized by molecular/genomic profiling demonstrating significant differences among these subtypes (8-11). These molecular aberrations include alterations in *IDH1/2*, *FGFR2*, *PIK3CA*, *ERRB2*, *KRAS*, and *BRAF* genes. Clinical trials investigating novel agents targeting a variety of such alterations are showing promise (12-15).

Furthermore, chronic inflammation plays an important role in the carcinogenesis of BTC, highlighting the immune system's role in this disease and in the potential for immunotherapy as a therapeutic option for patients with BTC. However, limited information is available regarding the immune microenvironment and the role immunotherapy plays in patients with BTC.

Programmed death ligand-1 (PD-L1) and programmed death-1 (PD-1) expression has been shown to be associated with a response to immunotherapy in a number of malignancies. This relationship is not definitive in predicting response to therapeutic PD-1 or PD-L1 blockade, but provides a rationale to study this further in patients with cholangiocarcinoma. A limited cohort of studies have documented high expression of PD-1 and PD-L1 in BTC cell lines and mouse models of BTC, suggesting that these immune checkpoint proteins may play a role in tumor progression (16).

Thus far studies targeting the PD-1/PD-L1 immune checkpoints have shown modest results in BTC. The KEYNOTE-028 and KEYNOTE-158 trials are the biggest cohorts to date utilizing immunotherapy, more specifically the PD-1 antibody, pembrolizumab (17). Both trials studied single agent pembrolizumab in patients with advanced BTC which progressed on standard line therapies. KEYNOTE-028 included 24 patients, all PD-L1 positive (defined as membranous PD-L1 expression in ≥1% of tumor and associated inflammatory cells or positive staining stroma) and showed an overall response rate (ORR) of 13%, mPFS 1.8 months, and mOS 6.2 months. KEYNOTE-158 evaluated 104 BTC patients, 58.6% were positive for PD-L1. The ORR was 5.8% (one of the responses was in a PD-L1 negative tumor) while mPFS and mOS was 2 and 7.4 months, respectively. Additionally a phase II study utilizing another PD-1 antibody, nivolumab, was studied in 54 patients with advanced BTC after progression on standard line therapy (18). The ORR was 22% with associated mPFS and mOS of 3.9 and 14.2 months, respectively. PD-L1 status will be reported at a later date.

Kelley and colleagues reported on a trial of pembrolizumab plus granulocyte macrophage colony stimulating factor (GM-CSF) in patients with advanced BTC (19). A total of 27 patients with heavily pre-treated intrahepatic/extra-hepatic BTC (74%/26%) were enrolled. The vast majority of patients (70%) had mismatch repair stable (MSS) disease; 41% of patients had low tumor mutation burden (TMB) and 41% had unknown TMB status. Confirmed partial response rate was 19% [1 microsatellite instability high (MSI-H), 4 MSS], with 33% of patients having maintained a partial response or stable disease for more than 6 months. Median OS had not yet been reached at the time of data presentation. PD-L1 positive disease (defined as PD-L1 staining in ≥1% of cells in tumor nests) was found in 30% of patients' pre-treatment, but was not associated with improved overall response or progression-free survival.

Ongoing studies in BTC are investigating different strategies to augment the immune system by a number of mechanisms, including CTLA-4 and PD-1 blockade (NCT02834013), PD-L1 and MEK inhibition (NCT03201458), tyrosine kinase inhibitors with PD-1 blockade (NCT03797326), histone deacetylase inhibitors with PD-L1 blockade (NCT03257761). Our work may be relevant to these new combinatorial strategies as information regarding the association of molecular alterations with PD-1/PD-L1 expression may predict for benefit from immune stimulation.

The aims of this study were the following: (I) to evaluate the expression of PD-1 and PD-L1 in a large cohort of samples of BTCs collected from multiple locations, and (II)

to assess for associations between PD-1/PD-L1 expression status and any particular genomic alterations. The latter could serve as a basis for further work on potential combinatorial, personalized therapies.

Methods

Patients and multiplatform molecular profiling

This study includes data from patients with BTC assayed by at least 1 platform [immunohistochemistry (IHC), in situ hybridization (ISH), and next-generation sequencing (NGS)] by Caris Life Sciences. All patients had to have reported PD-L1 expression by IHC for inclusion into the study. Formalin-fixed paraffin-embedded (FFPE) tumor samples were sent by treating physicians for analysis. All tumor samples were verified by board-certified pathologists for sufficient tumor content, specimen quality, and confirmation of diagnosis. The testing performed for each patient have varied based on the physician's request, tissue availability, and technical requirements for data to be reported.

Validation and institutional review board

All methods utilized in this study were clinically validated to at least Clinical Laboratory Improvement Amendments, College of American Pathologists, and International Organization for Standardization (ISO) 15189. This retrospective analysis utilized previously collected de-identified data created under the Caris honest broker policy and followed consultation with the Western Institutional Review Board (IRB), which is the IRB of record for Caris Life Sciences. The project was deemed exempt from IRB oversight and consent requirements were waived.

NGS

Specimens were profiled using massively parallel NGS sequencing using the SureSelect XT enrichment kit of biotinylated RNA probes to capture DNA fragments from the exons of 592 genes (Agilent, Santa Clara, CA). Enriched libraries were the sequenced on the Illumina NextSeq instrument (Illumina, San Diego, CA). All variants reported are detected with >99% confidence (based on mutation frequency and amplicon coverage) with an average sequencing depth of >1,000 X. Copy number alterations (CNA) were also explored on samples by NGS for 442

genes. CNAs were calculated by comparing the depth of sequencing of genomic loci to a diploid control as well as the known performance of these genomic loci. Gains ≥6 copies were considered amplified.

Tumor mutational burden (TMB) was calculated by counting nonsynonymous missense mutations and excluding common germline variants. TMB was considered high if ≥17 mutations (mut)/megabase (Mb) were detected. The threshold for determining high TMB (defined as ≥17 mut/Mb) was established by comparing TMB with microsatellite instability (MSI) by fragment analysis in colorectal cancer cases; based on reports of TMB having high concordance with MSI in colorectal cancer (20). MSI was calculated from the NGS data by direct analysis of short tandem repeat tracts in the target regions of sequenced genes. The count only included alterations that resulted in increases or decreases in the number of repeats; MSI-H was defined as ≥46 altered microsatellite loci (the threshold was established by comparing NGS to the PCR-based microsatellite fragments analysis results from ~2,100 cases) (20).

IHC

IHC analysis of 24 proteins was performed on FFPE tumor samples using commercially available detection kits and automated staining techniques (Benchmark XT; Ventana Medical Systems, Tucson, AZ; and Autostainer-Link 48; Dako, Carpinteria, CA). Antibody clones used are provided in Supplementary Methods. Appropriate positive and negative controls were used for all proteins tested. IHCs were scored manually by board-certified pathologists using predefined thresholds consisting of intensity of staining (0, 1+, 2+, and 3+) and percentage of tumor cells that stained positive. Thresholds are derived from peer-reviewed clinical literature, which associates response to treatment to biomarker status (21,22). Tests are interpreted as positive or negative, and the expression data are represented as a distribution (percentage) of positive or negative results observed in the cohort tested. PD-1 [NAT105 antibody; ≥1+ staining of tumor infiltrating lymphocytes (TILs) considered positive] and PD-L1 (SP142 antibody; ≥2+ and ≥5% staining in tumor cells considered positive) status was tested in all samples.

ISH

Gene CNAs of *cMET*, *EGFR*, *HER2*, *PIK3CA*, and *TOP2A*

Table 1 Demographics characteristics for participants included in the study

Clinical parameters	ECC	GBC	ICC	ECC + GBC	Total	P
Number	77	203	372	280	652	
Age (years)						0.08
Mean	66	64	63	65	64	
Range	34–88	33–85	28–88	33–88	28–88	
Sex, n [%]						0.07
Female	29 [38]	138 [68]	192 [52]	167 [60]	362 [56]	
Male	48 [62]	65 [32]	177 [48]	113 [40]	290 [44]	

P values were calculated by comparing ICC to the ECC + GBC combined group. Age was compared using a *t*-test and sex was compared using a Chi-squared test. ECC, extrahepatic cholangiocarcinoma; GBC, gallbladder cancer; ICC, intrahepatic cholangiocarcinoma.

were analyzed in a subset of patients by DNA ISH using fluorescence ISH and/or chromogenic ISH probes as part of the automated staining techniques (Benchmark XT; Ventana Medical Systems) and automated imaging systems (BioView, Billerica, MA). Cutoffs are provided in the *Table S1*. The ratio of gene to peri-centromeric regions of chromosome 7 (EGFR, cMET), 17 (HER2, TOP2A), and 3 (PIK3CA) were used to determine increases in gene copy number. Ratios higher than the defined cutoff were considered positive and ratios less than defined cutoff were considered negative.

Statistical methods

Demographic and genomic predictors were compared across BTC subtypes and between PD-L1 positive and negative groups. Numeric predictors were assessed using *t*-tests. Categorical predictors were assessed using Chi-squared test or Fisher's exact test where appropriate. Adjusted P-values were calculated using the Benjamini and Hochberg method. All statistical tests were two-sided with alpha level set at 0.05 for statistical significance. To predict the TMB threshold that would discriminate PD-L1 positive from PD-L1 negative cases, ROC curve analysis was generated using the pROC package in Rusing the Youden's J statistic (23).

Results

Patient demographics

Samples from a total of 652 patients with BTC were included in this study, including 77 extrahepatic cholangiocarcinoma (ECC), 203 GBC, and 372 intrahepatic

cholangiocarcinoma (ICC). Demographics are seen in *Table 1*. Females represented 38%, 68%, and 52% of the populations, respectively. Median age of patients was 67 years old (range, 34–88 years old), 65 years old (range, 33–85 years old), and 64.5 years old (range, 28–88 years old), respectively. While increasing age and female gender appear more associated with ECC as compared to ICC, the differences did not reach statistical significance (P=0.078 and P=0.067, respectively).

PD-L1 and PD-1 positivity

PD-L1 results, detailed in *Table 2*, were evaluable for 77 ECC, 203 GBC, and 372 ICC. PD-L1 expression (on tumor cells) was 5%, 12%, and 7%, respectively. This led to an overall PD-L1 positive rate of 8.6% (56/652). PD-1 expression (on TILs) was present in 43%, 55%, and 53%, respectively. This led to an overall PD-1 positive rate of 49% (36/73). There was no correlation between PD-L1 status and primary tumor location (P=0.203) or gender (P=0.780), however the average age of PD-L1 negative patients was statistically older than PD-L1 positives (mean 64.2 *vs.* 60.7 years; P=0.046).

Gene mutations

The prevalence of genomic mutations is described in *Table 3*. Mutations with the highest prevalence among the group of BTCs as a whole included: *TP53* (n=255, 41.8%), *ARID1A* (n=106, 37.3%), *KRAS* (n=109, 17.6%), *CDKN2A* (n=50, 8.6%), *IDH1* (n=50, 8.1%), *SMAD4* (n=46, 7.4%), *BAP1* (n=42, 6.8%), and *PIK3CA* (n=35, 5.7%). A total of nine FGFR2 fusions, with various binding partners, were

Table 2 Rates of PD-1 and PD-L1 positivity in BTCs

Clinical parameters	ECC	GBC	ICC	ECC + GBC	Total	P
Number	77	203	372	280	652	
IHC PD-L1, n [%]						0.16
Positive	4 [5]	25 [12]	27 [7]	29 [10]	56 [9]	
Negative	73 [95]	178 [88]	345 [93]	251 [90]	596 [91]	
IHC PD-1, n [%]						0.56
Positive	3 [43]	16 [55]	17 [53]	19 [53]	36 [49]	
Negative	4 [57]	13 [45]	20 [54]	17 [47]	37 [51]	

ECC, extrahepatic cholangiocarcinoma; GBC, gallbladder cancer; ICC, intrahepatic cholangiocarcinoma; PD-1, programmed death-1; PD-L1, programmed death ligand-1; BTC, biliary tract cancer; IHC, immunohistochemistry.

identified but none were detected in a PD-L1 positive tumor. Fusions were also detected involving FGFR3 and BRAF.

TMB

Overall the mean TMB for the entire cohort was 7.2 mutations (mut)/megabase (Mb). Mean TMB in the PD-L1 positive group was statistically significantly higher (10 *vs.* 6.9 mut/Mb in the PD-L1 negative group (P=0.002). This pattern held true across ICC and ECC/GBC location types. In the ICC group, PD-L1 positive samples had a TMB mean of 10.7 mut/Mb as compared to mean of 6.5 mut/Mb (P=0.12) in PD-L1 negative tumors. In extrahepatic and gallbladder subtypes together, TMB mean was 9.4 mut/Mb in PD-L1 positive tumors as compared to a mean of 7.4 mut/Mb (P=0.06) in PD-L1 negative tumors. A ROC curve was generated using TMB as a predictor for PD-L1 status (*Figure S1*). The best TMB threshold to differentiate PD-L1 positive from negative cases was 6.5 mut/Mb. Using this threshold generated an area under the curve (AUC) of 0.639, which corresponded to 58.5% sensitivity and 62.5% specificity.

PD-L1 and gene mutation associations

The rate of clinically relevant and/or potentially targetable mutations in the samples with PD-L1 positivity (details based on location noted in *Table S1*) were: *ARID1A* (11/22, 50%), *ATM* (2/54, 3.7%), *BAP1* (2/56, 3.6%), *BRAF* [5/56 (4 *V600E*, 1 *D594N*), 8.9%], *BRCA1* (1/54, 1.9%), *BRCA2* (5/55, 9.1%), *CDKN2A* (6/51, 11.8%), *ERBB2* (1/56, 1.8%), *IDH1* (1/56, 1.8%), *IDH2* (1/56, 1.8%), *JAK1* (1/53, 1.9%),

KRAS (13/56, 23.2%), *MAP2K* (2/56, 3.6%), *MSH2* (1/53, 1.9%), *NF1* (4/51, 7.8%), *NRAS* (3/56, 5.4%), *PALB2* (1/55, 1.8%), *PIK3CA* (2/53, 3.8%), *RB1* (2/53, 3.8%), and *TP53* (35/56, 62.5%). Note that the denominator represents PD-L1 positive samples. Also note that 4 of the mutations that statistically correlated with PD-L1 expression, detailed in *Table 4*, were: *TP53* (P=0.001), *BRCA2* (P=0.02), *BRAF* (P=0.01), *GNAS* (P=0.004), *SMARCB1* (P<0.001), and *RNF43* (P=0.003). Additionally, both the genes that encode for the PDL1 and PDL2 proteins, CD274 and PDCD1LG2, were both amplified exclusively in PD-L1 expressing cohort (P<0.001 for both). Among additional biomarkers tested, TOP2A expression (IHC) (P=0.02), TMB high (≥17 mut/Mb) [10.7% (6/56); P=0.001], and MSI-H status [7.1% (4/56); P=0.001] were all shown to be statistically correlated with PD-L1 positivity.

Discussion

Immunotherapy in the form of checkpoint inhibitors (i.e., anti-PD-1/PD-L1 antibodies) alone and in combination with chemotherapy, other immunotherapies, as well as targeted therapies are currently being employed in a variety of malignancies. An observation and rationale for why immunotherapy may be effective in BTC is based on the observation that tumor infiltration by the cellular mediators of the adaptive immune response such as CD8+ and CD4+ cells is generally correlated with improved outcomes in BTC (24,25). This improved prognosis suggests that CD4+ and CD8+ T cells infiltrating cholangiocarcinoma may be functioning to delay tumor progression, thus harnessing and augmenting this T-cell response may provide clinical benefit. Conversely, there is data that PD-1

1104

Mody et al. PD-L1 expression correlates in BTC

Table 3 Genomic alterations among BTCs

Gene	Number of aberrant cases/total tested	Alteration as a % of cases (95 exact binomial CI)
Gene with mutation present		
TP53	255/610	41.8 (37.9–45.8)
ARID1A	106/284	37.3 (31.7–43.2)
KRAS	109/621	17.6 (14.6–20.8)
CDKN2A	50/583	8.6 (6.4–11.2)
IDH1	50/621	8.1 (6.0–10.5)
SMAD4	46/620	7.4 (5.5–9.8)
BAP1	42/620	6.8 (4.9–9.0)
PIK3CA	35/617	5.7 (4.0–7.8)
PBRM1	28/615	4.6 (3.0–6.5)
APC	26/620	4.2 (2.8–6.1)
NF1	20/552	3.6 (2.2–5.5)
BRCA2	22/615	3.6 (2.3–5.4)
ARID2	21/603	3.5 (2.2–5.3)
ATM	21/616	3.4 (2.1–5.2)
BRAF	21/620	3.4 (2.1–5.1)
IDH2	20/621	3.2 (2.0–4.9)
NRAS	20/621	3.2 (2.0–4.9)
RNF43	12/620	1.9 (1.0–3.4)
CHEK2	10/550	1.8 (0.9–3.3)
CTNNB1	11/619	1.8 (0.9–3.2)
PTEN	10/588	1.7 (0.8–3.1)
RB1	9/592	1.5 (0.7–2.9)
ERBB2	9/621	1.4 (0.7–2.7)
PALB2	8/620	1.3 (0.6–2.5)
ERBB3	8/621	1.3 (0.6–2.5)
WRN	6/530	1.1 (0.4–2.4)
Gene with copy number amplified		
ERBB2	19/591	3.2 (1.9–5.0)
MDM2	19/591	3.2 (1.9–5.0)
MYC	16/591	2.7 (1.6–4.4)
CCND1	12/591	2.0 (1.1–3.5)
FGF19	11/575	1.9 (1.0–3.4)
WIF1	6/575	1.0 (0.4–2.3)
MCL1	6/591	1.0 (0.4–2.2)

BTC, biliary tract cancer.

expression on TILs contributes to an immunosuppressive environment (26). In our analysis we found that of the samples tested 49% (36/73) had TILs considered PD-1 positive. Checkpoint inhibition, namely PD-1 blockade, in cholangiocarcinoma has been largely disappointing. Data from the KEYNOTE-158, KEYNOTE-028, and nivolumab studies represents the largest cohort of patients with BTC treated with PD-1 antibodies and the results were modest at best (see Introduction).

It remains unclear how the adaptive immune resistance pathway plays a role in BTC and whether these novel immunotherapies might eventually be effective in patients with BTC. Several immunotherapeutic strategies targeting BTC have been or are currently being investigated such as peptide and dendritic cell vaccines targeting overexpressed tumor antigens, cytokine therapies, adoptive T-cell therapy, and checkpoint inhibitors (27). In general, there have been hints of clinical activity in a small number of patients

Further, there are limited data evaluating PD-1 and PD-L1 expression in small cohorts of patients' BTC tumor samples, and these studies report high positivity rates. A study of 31 resected intrahepatic BTCs in China showed that 100% of cases demonstrated PD-L1 positivity (28). This study evaluated PD-L1 staining of tumor cells and intensity of overall staining over 5 high-powered magnification fields at the "hot spot in a cancer area". Staining intensity was graded as: negative staining, light (<25% cells stained), moderate (25–50% cells stained), or intense (>50% stained cells). PD-L1 sensitivity, defined as at least mild staining on plasma membrane or cytoplasm of tumor cells, was noted in all 31 ICC cases.

Another study looking at 70 specimens of extrahepatic BTCs revealed a PD-L1 positivity of 43% (29). This study showed that PD-L1 positivity (defined as IHC ≥3+ staining) was associated with a worse prognosis on multivariate analysis. Fontugne et al. looked at PD-L1 expression on tumor cells in perihilar and intrahepatic BTC, with positivity defined as ≥5% staining (30). They noted a PDL-L1 positivity rate of only 9%, although this number increased to 46% when including PD-L1 positive surrounding inflammatory cells. Further, Gani et al. examined PD-L1 (monoclonal antibody 5H1; ≥5% staining considered positive) specifically on the neoplastic cells of intrahepatic BTC from 54 patients undergoing surgery at a single center, revealing a 72% PD-L1positivity rate (31). Our study shows strikingly different results in the largest cohort thus far reported in the literature evaluating PD-L1 staining, with PD-L1 positivity in 12% of GBC, 7% of

Table 4 PD-L1 positivity based on genomic alteration

Genomic alteration	Mutation present/total PD-L1 + cases profiled (%)	Mutation present/total PD-L1 – cases profiled (%)	P value	Q value
Gene with mutation				
ARID1A	11/22 (50.0%)	95/262 (36.3%)	0.20	0.80
ARID2	4/54 (7.4%)	17/549 (3.1%)	0.09	0.72
ATM	2/54 (3.7%)	19/562 (3.4%)	0.90	0.91
BAP1	2/56 (3.6%)	40/564 (7.1%)	0.31	0.80
BRAF	5/56 (8.9%)	16/564 (2.8%)	0.01	0.16
BRCA1	1/54 (1.9%)	3/561 (0.5%)	0.25	0.80
BRCA2	5/55 (9.1%)	17/560 (3.0%)	0.02	0.20
CDKN2A	6/51 (11.8%)	44/532 (8.3%)	0.39	0.80
ERBB2	1/56 (1.8%)	8/565 (1.4%)	0.82	0.84
ERBB3	2/56 (3.6%)	6/565 (1.1%)	0.11	0.79
GNAS	2/56 (3.6%)	2/565 (0.4%)	0.004	0.05
IDH1	1/56 (1.8%)	49/565 (8.7%)	0.07	0.54
IDH2	1/56 (1.8%)	19/565 (3.4%)	0.52	0.80
JAK1	1/53 (1.9%)	0/551 (0.0%)	0.001	0.02
KRAS	13/56 (23.2%)	96/565 (17.0%)	0.24	0.80
PALB2	1/56 (1.8%)	7/564 (1.2%)	0.73	0.80
PIK3CA	2/55 (3.6%)	33/562 (5.9%)	0.49	0.80
RB1	2/53 (3.8%)	7/539 (1.3%)	0.16	0.80
RNF43	4/56 (7.1%)	8/564 (1.4%)	0.003	0.04
SMARCB1	2/56 (3.6%)	0/564 (0.0%)	<0.001	0.001
TP53	35/56 (62.5%)	220/554 (39.7%)	0.001	0.02
Copy number variant amplified				
CD274 (PDL1 gene)	1/49 (2.0%)	0/525 (0.0%)	0.001	0.02
EGFR	2/53 (3.8%)	2/538 (0.4%)	0.004	0.05
ERBB2	2/53 (3.8%)	17/538 (3.2%)	0.81	0.83
FGF19	1/49 (2.0%)	10/526 (1.9%)	0.94	0.94
MET	3/53 (5.7%)	6/538 (1.1%)	0.01	0.11
PDCD1LG2 (PDL2 gene)	2/49 (4.1%)	0/524 (0.0%)	<0.001	<0.001
IHC loss				
MLH1	1/5 (20.0%)	4/61 (6.6%)	0.27	0.80
MSH2	1/5 (20.0%)	0/61 (0.0%)	<0.001	0.02
MSH6	1/5 (20.0%)	0/59 (0.0%)	0.001	0.02
PMS2	1/5 (20.0%)	4/59 (6.8%)	0.29	0.80

Table 4 (*Continued*)

Table 4 (*Continued*)

Genomic alteration	Mutation present/total PD-L1 + cases profiled (%)	Mutation present/total PD-L1 – cases profiled (%)	P value	Q value
IHC expression				
TOP2A	9/9 (100.0%)	61/98 (62.2%)	0.02	0.21
Other				
TMB high*	6/56 (10.7%)	13/556 (2.3%)	0.001	0.02
MSI-H	4/56 (7.1%)	9/552 (1.6%)	0.007	0.07

*, TMB high defined as ≥17 mut/Mb. PD-L1, programmed death ligand-1; TMB, tumor mutational burden.

ICC, and 5% of ECC.

In recent years, genomic profiling of BTCs has revealed it to be a diverse and heterogeneous disease (8,9,11). The identification of molecular subtypes of this disease has led to some measures of success with particular targeted therapies in patients, particularly those with FGFR2 fusions, mutations in IDH1, BRAF, and amplifications of HER2 (12-15). As it relates to the study reported herein, we sought to explore whether certain genomic alterations were associated with increased PD-L1 positivity rates. This line of inquiry is novel in this disease and particularly relevant with genes involved in the DNA damage response (DDR). As such if a cell has a defect in its ability to repair DNA then mutations accumulate. This accumulation of mutations can be measured and referred to as the TMB, or tumor mutational load (TML), which is defined as the number of genetic variants per megabase of DNA. As more mutations are acquired, more neoantigens are expressed and a tumor that was previously undetectable by the immune system can now be potentially recognized and targeted immunologically. To help facilitate this anti-neoplastic immune activity, immune checkpoint inhibitors can be employed. The use poly (ADP) ribose polymerase (PARP) inhibitors combined with immunotherapy highlights the approach of exploiting DNA repair inhibition to augment the immune system. There are currently over 200 clinical trials of DDR targeting agents and immunotherapy across a multitude of malignancies (32). One such trial is a phase II study of the PARP inhibitor, rucaparib, in combination with nivolumab in patients with advanced BTCs (NCT03639935).

Of potential clinical significance, as related to the intersection of genomic alterations, specifically in DDR, and immunotherapy is our finding of a statistically significant increased frequency of BRCA2 mutations among PD-L1 positive BTCs. Along those lines there is recent data to suggest increased PD-L1 expression in gastroesophageal cancers with DDR mutations (33). There are ongoing clinical trials studying immunotherapy (i.e., checkpoint inhibitors) and PARP inhibition in patients with DDR deficiency (such as BRCA mutation) (NCT02657889, NCT02953457, NCT02571725).

We also reveal an increased frequency of PD-L1 expression (23%) in KRAS mutated BTC. This is one of the more frequent mutations present in BTC (34). Though KRAS is not directly targetable, MEK inhibition has emerged as a logical target given that KRAS mutation causes downstream dysregulation and activation of the Raf-MEK-ERK pathway. Additionally, there is evidence that MEK activity can lead to an immunosuppressive tumor microenvironment, in part, by suppressing transcription of MHC-1 components (35). MEK inhibition also upregulates tumor major histocompatibility complex-I expression and promotes intratumoral T-cell accumulation. Based on these principles, there is a clinical trial investigating the use of atezolizumab (PD-L1 antibody) +/– cobimetinib (MEK inhibitor) in BTC (NCT03201458) which has recently completed accrual.

Our data also reveal a statistically significant association between BRAF mutations and PD-L1 positivity. In a preclinical syngeneic mouse model using $BRAF^{V600E}$ mutated melanoma cells, both dual and individual inhibition of BRAF and MEK resulted in increased T cell recruitment around the tumor. Additionally, BRAF inhibition was found to result in PD-L1 expression suggesting an adaptive immune resistance mechanism by effector T-cells. The combination of adoptive cell transfer (i.e., immunotherapy) along with BRAF/MEK inhibition in this same model resulted in superior antitumor activity (36). This set the stage for KEYNOTE-022 which confirmed the safety of

pembrolizumab, dabrafenib, and trametinib for metastatic BRAF-mutated melanoma. This led to a phase II trial of the same name (NCT02130466) and two randomized placebo-controlled phase III trials testing BRAF/MEK inhibition +/– immunotherapy (NCT02908672, NCT02967692) studying this approach.

TMB is evolving as another surrogate marker for response to immunotherapy, outside of the traditional biomarkers for response to immunotherapy [e.g., microsatellite instability high (MSI-H), PD-L1 positivity]. The CheckMate-586 trial studied non-small cell lung cancer patients being treated with first-line nivolumab and ipilimumab. The study evaluated overall survival stratified by TMB as a secondary endpoint (37). The results revealed that patients with a TMB of ≥10 mut/Mb (assessed by Foundation One CDx) had an objective response rate of 44% as compared to 9–15% for TMB <10 mut/Mb. Additionally, the progression-free survival (PFS) was 7.1 months with TMB ≥10 mut/Mb as compared to 2.6 months with TMB <10 mut/Mb (38). Jain *et al.* reported on TMB in BTCs and found that 15% (n=9) of tumors were TMB high (defined as ≥20 mut/Mb) and 85% (n=51) were defined as TMB intermediate (defined as 6–19 mut/Mb) (39). Our analysis revealed an association of increased TMB with PD-L1 positivity, with a mean TMB of 10 mut/Mb in the PD-L1 positive group versus 6.9 mut/Mb in the PDL-1 negative group (P=0.002). Taking as a whole our findings suggest a correlation of PD-L1 and TMB which could have implications for treatment with checkpoint inhibitors (i.e., PD-1/PD-L1 inhibitors) in this subset of patients.

Limitations of our study include the retrospective nature of the analysis along with the lack of clinical data to correlate with molecular findings. Further, the clinical heterogeneity of the data is a limitation, such that some of the tissue samples were from primary tumor or others from metastatic lesions. Lastly, not all of the samples were able to be processed for mutational status, copy number variation, and/or IHC expression. For example, only 22 of the 56 PD-L1 positive cases were able to be analyzed for ARID1A mutations. This was secondary to the amount of tissue available.

Conclusions

In summary, we report on the largest cohort of BTCs to date an analysis of PD-L1 status, the association between PD-L1 positivity and particular genetic aberrations, and TMB status in BTC. Such associations have not previously been reported upon. PD-L1 expression on tumor cells was highest in patients with GBC followed by intrahepatic and ECC. Of the PD-L1 positive tumors (n=56) the most frequent genomic alterations include: TP53 (P=0.001), KRAS, ARID1A, CDK2NA, BRCA2 (P=0.02), BRAF (P=0.016), and RNF43 (P=0.04). Further, the presence of TMB high (defined as ≥17 mut/Mb) (P=0.001), MSI-H (P=0.007), and TOP2A IHC (P=0.02) expression showed a statistically significant increase in PD-L1 expression. Our hope is that these findings could help generate hypotheses to understand which subsets of cholangiocarcinoma could preferentially respond to immunotherapy, and to develop studies of regimens combining particular targeted therapies with immunotherapies.

Acknowledgments

Footnote

Conflicts of Interest: K Mody—Research Support: Agios, Senwha Biosciences, Taiho, ArQule, AstraZeneca, Genentech, Incyte, Tracon Pharmaceuticals, Medimmune, Puma Biotechnology. Consulting: Astra Zeneca, Bayer, Celgene, Eisai, Exelixis, Ipsen, Merrimack, Vicus. M Saul and K Poorman—Employment: Caris Life Sciences. The other authors have no conflicts of interest to declare.

Ethical Statement: The authors are accountable for all aspects of the work in ensuring that questions related to the accuracy or integrity of any part of the work are appropriately investigated and resolved. The project was deemed exempt from IRB oversight and consent requirements were waived.

References

1. Marzioni M, Invernizzi P, Candelaresi C, et al. Human cholangiocarcinoma development is associated with dysregulation of opioidergic modulation of cholangiocyte growth. Dig Liver Dis 2009;41:523-33.
2. Ayala D, Blackstock AW. Effective treatment strategies for

1108

Mody et al. PD-L1 expression correlates in BTC

cholangiocarcinoma: the challenge remains. Gastrointest Cancer Res 2008;2:251-2.

3. Cardinale V, Semeraro R, Torrice A, et al. Intra-hepatic and extra-hepatic cholangiocarcinoma: New insight into epidemiology and risk factors. World J Gastrointest Oncol 2010;2:407-16.

4. Patel T. Increasing incidence and mortality of primary intrahepatic cholangiocarcinoma in the United States. Hepatology 2001;33:1353-7.

5. Patel T. Cholangiocarcinoma--controversies and challenges. Nat Rev Gastroenterol Hepatol 2011;8:189-200.

6. Alvaro D, Crocetti E, Ferretti S, et al. Descriptive epidemiology of cholangiocarcinoma in Italy. Dig Liver Dis 2010;42:490-5.

7. Valle J, Wasan H, Palmer DH, et al. Cisplatin plus gemcitabine versus gemcitabine for biliary tract cancer. N Engl J Med 2010;362:1273-81.

8. Chan-On W, Kuwahara K, Kobayashi N, et al. Cholangiocarcinomas associated with long-term inflammation express the activation-induced cytidine deaminase and germinal center-associated nuclear protein involved in immunoglobulin V-region diversification. Int J Oncol 2009;35:287-95.

9. Churi CR, Shroff R, Wang Y, et al. Mutation profiling in cholangiocarcinoma: prognostic and therapeutic implications. PLoS One 2014;9:e115383.

10. Putra J, de Abreu FB, Peterson JD, et al. Molecular profiling of intrahepatic and extrahepatic cholangiocarcinoma using next generation sequencing. Exp Mol Pathol 2015;99:240-4.

11. Ross JS, Wang K, Javle MM, et al. Comprehensive genomic profiling of biliary tract cancers to reveal tumor-specific differences and genomic alterations. J Clin Oncol 2015;33:231.

12. Javle M, Lowery M, Shroff RT, et al. Phase II Study of BGJ398 in Patients With FGFR-Altered Advanced Cholangiocarcinoma. J Clin Oncol 2018;36:276-82.

13. Lowery MA, Abou-Alfa GK, Burris HA, et al. Phase I study of AG-120, an IDH1 mutant enzyme inhibitor: Results from the cholangiocarcinoma dose escalation and expansion cohorts. J Clin Oncol 2017;35:4015.

14. Javle M, Churi C, Kang HC, et al. HER2/neu-directed therapy for biliary tract cancer. J Hematol Oncol 2015;8:58.

15. Wainberg ZA, Lassen UN, Elez E, et al. Efficacy and safety of dabrafenib and trametinib in patients with BRAF V600E-mutated biliary tract cancer: A cohort of the ROAR basket trial. J Clin Oncol 2019;37:187.

16. Tamai K, Nakamura M, Mizuma M, et al. Suppressive expression of CD274 increases tumorigenesis and cancer stem cell phenotypes in cholangiocarcinoma. Cancer Sci 2014;105:667-74.

17. Bang Y, Ueno M, Malka D, et al. Pembrolizumab (pembro) for advanced biliary adenocarcinoma: Results from the KEYNOTE-028 (KN028) and KEYNOTE-158 (KN158) basket studies. J Clin Oncol 2019;37:4079.

18. Kim R, Kim D, Alese O, et al. A phase II study of nivolumab in patients with advanced refractory biliary tract cancers (BTC). J Clin Oncol 2019;37:4097.

19. Kelley RK, Mitchell E, Behr S, et al. Phase 2 trial of pembrolizumab (PEM) plus granulocyte macrophage colony stimulating factor (GM-CSF) in advanced biliary cancers (ABC): Clinical outcomes and biomarker analyses. J Clin Oncol 2018;36:4087.

20. Vanderwalde A, Spetzler D, Xiao N, et al. Microsatellite instability status determined by next-generation sequencing and compared with PD-L1 and tumor mutational burden in 11,348 patients. Cancer Med 2018;7:746-56.

21. Smyth MJ, Ngiow SF, Ribas A, et al. Combination cancer immunotherapies tailored to the tumour microenvironment. Nat Rev Clin Oncol 2016;13:143-58.

22. Herbst RS, Soria JC, Kowanetz M, et al. Predictive correlates of response to the anti-PD-L1 antibody MPDL3280A in cancer patients. Nature 2014;515:563-7.

23. Robin X, Turck N, Hainard A, et al. pROC: an open-source package for R and S+ to analyze and compare ROC curves. BMC Bioinformatics 2011;12:77.

24. Goeppert B, Frauenschuh L, Zucknick M, et al. Prognostic impact of tumour-infiltrating immune cells on biliary tract cancer. Br J Cancer 2013;109:2665-74.

25. Oshikiri T, Miyamoto M, Shichinohe T, et al. Prognostic value of intratumoral CD8+ T lymphocyte in extrahepatic bile duct carcinoma as essential immune response. J Surg Oncol 2003;84:224-8.

26. Ahmadzadeh M, Johnson LA, Heemskerk B, et al. Tumor antigen-specific CD8 T cells infiltrating the tumor express high levels of PD-1 and are functionally impaired. Blood 2009;114:1537-44.

27. Marks EI, Yee NS. Immunotherapeutic approaches in biliary tract carcinoma: Current status and emerging strategies. World J Gastrointest Oncol 2015;7:338-46.

28. Ye Y, Zhou L, Xie X, et al. Interaction of B7-H1 on intrahepatic cholangiocarcinoma cells with PD-1 on tumor-infiltrating T cells as a mechanism of immune evasion. J Surg Oncol 2009;100:500-4.

29. Suleiman Y, Coppola D, Zibadi S, et al. Prognostic value

of tumor-infiltrating lymphocytes (TILs) and expression of PD-L1 in cholangiocarcinoma. J Clin Oncol 2015;33:295.

30. Fontugne J, Augustin J, Pujals A, et al. PD-L1 expression in perihilar and intrahepatic cholangiocarcinoma. Oncotarget 2017;8:24644-51.

31. Gani F, Nagarajan N, Kim Y, et al. Program Death 1 Immune Checkpoint and Tumor Microenvironment: Implications for Patients With Intrahepatic Cholangiocarcinoma. Ann Surg Oncol 2016;23:2610-7.

32. Brown JS, Sundar R, Lopez J. Combining DNA damaging therapeutics with immunotherapy: more haste, less speed. Br J Cancer 2018;118:312-24.

33. Cerniglia M, Xiu J, Grothey A, et al. Association of DNA damage response and repair genes (DDR) mutations and microsatellite instability (MSI), PD-L1 expression, tumor mutational burden (TMB) in gastroesophageal cancers. J Clin Oncol 2019;37:60.

34. Javle M, Bekaii-Saab T, Jain A, et al. Biliary cancer: Utility of next-generation sequencing for clinical management. Cancer 2016;122:3838-47.

35. Ebert PJR, Cheung J, Yang Y, et al. MAP Kinase Inhibition Promotes T Cell and Anti-tumor Activity in Combination with PD-L1 Checkpoint Blockade. Immunity 2016;44:609-21.

36. Hu-Lieskovan S, Mok S, Homet Moreno B, et al. Improved antitumor activity of immunotherapy with BRAF and MEK inhibitors in BRAF(V600E) melanoma. Sci Transl Med 2015;7:279ra41.

37. Ramalingam SS, Hellmann MD, Awad MM, et al. Tumor mutational burden (TMB) as a biomarker for clinical benefit from dual immune checkpoint blockade with nivolumab + ipilimumab in first-line, non-small cell lung cancer. Chicago, IL: AACR Annual Meeting, 2018.

38. Hellmann MD, Ciuleanu TE, Pluzanski A, et al. Nivolumab plus Ipilimumab in Lung Cancer with a High Tumor Mutational Burden. N Engl J Med 2018;378:2093-104.

39. Jain A, Shroff RT, Zuo M, et al. Tumor mutational burden (TMB) and co-existing actionable mutations in biliary tract cancers (BTC). J Clin Oncol 2017;35:4086.

IHC

IHC was performed on full FFPE sections of glass slides using commercially available detection kits and automated staining techniques optimized and validated per Clinical Laboratory Improvement Amendments (CLIA), College of American Pathologists (CAP), and International Organization for Standardization (ISO) requirements. Staining was scored for intensity (0: no staining; 1+: weak staining; 2+: moderate staining; 3+: strong staining) and staining percentage (0–100%). Results were categorized as positive or negative by defined thresholds specific to each marker based on published clinical literature that associates biomarker status with patient responses to therapeutic agents. A board-certified pathologist evaluated all IHC results independently. The following antibodies were evaluated: Androgen receptor (AR27), estrogen receptor (ER-SP1), human epidermal growth factor receptor 2 (Her2-4B5), DNA excision repair protein (ERCC1-8F1), O(6)-methylguanine-methyltransferase (MGMT-MT23.3), P-glycoprotein (PGP-C494), progesterone receptor (PR-1E2/100), phosphatase and tensin homolog (PTEN-6H2.1), ribonucleotide reductase M1 (RRM1-polyclonal), serum protein acidic and rich in cysteine (SPARC monoclonal-12251), serum protein acidic and rich in cysteine (SPARC polyclonal), topoisomerases 1 (TOPO1-1D6), topoisomerases 1 and 2α (TOPO2α-3 F6), thymidylate synthase (TS106/4H4B1), MET proto-oncogene, receptor tyrosine kinase (cMET-SP44), tubulin beta-3 chain (TUBB3-polyclonal), transducin-like enhancer of split 3 (TLE3-polyclonal), programmed cell death protein 1 (NAT105 antibody; ≥1+ staining of TILs considered positive), and programmed death-ligand 1 (PD-L1-SP142 on tumor cells). Expression data are represented as a distribution (percentage) of positive or negative results observed in the cohort tested.

Table S1 PD-L1 positivity based on tumor location and genomic alteration

Genomic alteration	PD-L1+		P value	Q value
	ECC/GBC	ICC		
ARID1A	3	8	0.033	0.487
BAP1	1	1	0.959	0.971
BRAF	2	3	0.580	0.709
BRCA1	1	0	0.349	0.490
BRCA2	2	3	0.609	0.732
CDKN2A	5	1	0.112	0.487
IDH1	0	1	0.296	0.487
IDH2	1	0	0.330	0.487
JAK1	0	1	0.285	0.487
KRAS	7	6	0.865	0.971
PBRM1	1	1	0.959	0.971
RB1	2	0	0.173	0.487
RNF43	1	3	0.266	0.487
SMAD4	2	2	0.941	0.971
TP53	21	14	0.112	0.487

ECC, extrahepatic cholangiocarcinoma; PD-L1, programmed death ligand-1; GBC, gallbladder cancer; ICC, cholangiocarcinoma.
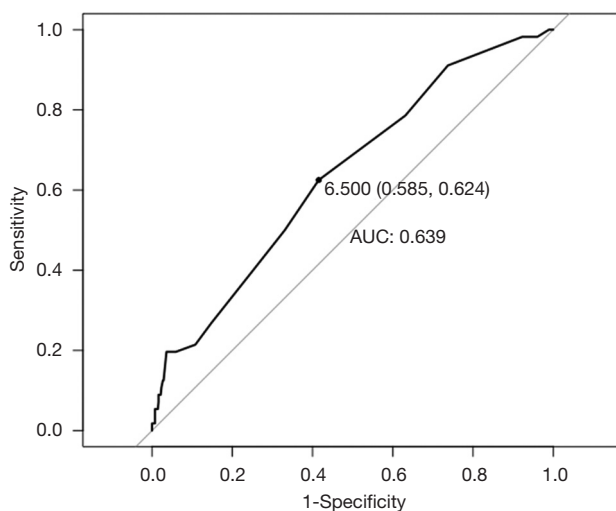
Figure S1 ROC curve analysis for TMB and PD-L1 expression. Evaluation of the threshold at which TMB can be used to predict PD-L1 status is calculated using Youden's J statistic. In this study, the best threshold to differentiate PD-L1 status corresponded to a TMB value of 6.5, which gave a specificity of 58.5%, and a sensitivity of 62.4%. PD-L1, programmed death ligand-1; TMB, tumor mutational burden.